The structure of an active acoustic metamaterial with tunable effective density

2009 New J. Phys. 11 123010

(http://iopscience.iop.org/1367-2630/11/12/123010)

New Journal of Physics
The open-access journal for physics

The structure of an active acoustic metamaterial with tunable effective density

A Baz
Mechanical Engineering Department, University of Maryland,
College Park, MD, USA
E-mail: baz@umd.edu

New Journal of Physics **11** (2009) 123010 (16pp)
Received 12 August 2009
Published 4 December 2009
Online at http://www.njp.org/
doi:10.1088/1367-2630/11/12/123010

Abstract. A new class of one-dimensional active acoustic metamaterials (AAMMs) with programmable effective densities is presented. The proposed AAMM is capable of producing densities that are orders of magnitudes lower or higher than the ambient fluid. Such characteristics are achieved by using an array of fluid cavities separated by piezoelectric diaphragms that are controlled to generate constant densities over wide frequency bands. The piezodiaphragms are augmented with passive electrical components to broaden the operating frequency bandwidth and enable densities higher than the fluid medium to be generated. The use of these components is shown to be essential to maintain the closed-loop compliance of the piezodiaphragm away from the zone of elastic instabilities. The values of the passive components are selected on a rational basis in order to ensure a balance between the frequency bandwidth and control voltage. With this unique structure of the AAMM, physically realizable acoustic cloaks can be implemented and objects treated with these active metamaterials can become acoustically invisible.

Contents

Nomenclature

A	area of cavity
C_C	compliance of cavity
C_D	open-loop compliance of diaphragm
C_{PB}	blocked capacitance of piezodiaphragm
C_{CD}	closed-loop compliance of diaphragm
C_S	tuning capacitance
D	electrical displacement
d_A	effective piezoelectric coefficient
E	electrical field
G	feedback gain
k	square root of the electro-acoustic coupling factor
L_C	inductance of cavity
L_P	tuning inductance
L	length of cavity
M_D	mass of diaphragm
p	fluid pressure in the time domain
P	fluid pressure in the Laplace domain
Δp	pressure drop along cavity
Δp_P	pressure across piezodiaphragm
Q	volumetric flow rate
q	electrical charge
S	strain
s^E	piezoelectric compliance
s	Laplace complex number
T	stress
t	diaphragm thickness

u	flow velocity
V	volume of cavity
V_{P}	piezoelectric voltage
Z_{P}	impedance of the piezodiaphragm and attached components

Greek symbols

ε	permittivity
κ	bulk's modulus of fluid
κ'	dimensionless bulk's modulus (κ/κ_0)
ρ	density of fluid
ρ'	dimensionless density (ρ/ρ_0)
ϕ	electro-acoustic transduction coefficient ($= -d_{\mathrm{A}}/C_{\mathrm{D}}$)
ω	frequency

Subscripts

d	desired
eff	effective
P	piezoelectric
0	ambient fluid

1. Introduction

Recently, interest has been focused on the development of various metamaterials with acoustical properties that are unachievable with natural materials. For example, composites of periodically distributed sonic scatterers are considered to produce acoustical properties, such as the sound speed and dynamical mass densities, that can be controlled by proper selection of the volume fraction, the elastic properties, positions in the unit cell, scattering interactions and refractive properties of the scatterers [1]–[6]. The resulting effective properties are highly dependent on the acoustic frequency range and can only be tuned for a narrow frequency band based on the arrangement of the sonic crystals. Other attempts include efforts to synthesize negative dynamic acoustical densities in fluid domains through the use of spring-mass lattice systems [7]–[10]. In these attempts, it was found that near a local resonant frequency, spatial decay of wave amplitude occurs as the effective mass becomes negative. Effective acoustic properties for poroelastic composites consisting of fluid matrix–solid constituents have also been investigated by Berryman [11] in order to predict the wave properties in the long wavelength limit.

Also, acoustic metafluids consisting of layered composite media have been considered. These metafluids have either anisotropic density and scalar bulk modulus [12] or anisotropic density and bulk modulus [13].

Unlike the extensive theoretical studies of acoustic metamaterials, experimental investigations are so far lacking. However, an important experimental study that is relevant to this paper is the work of Lee *et al* [14, 15] which demonstrated the negative effective density characteristics of an acoustic metamaterial consisting of an array of cavities separated by thin

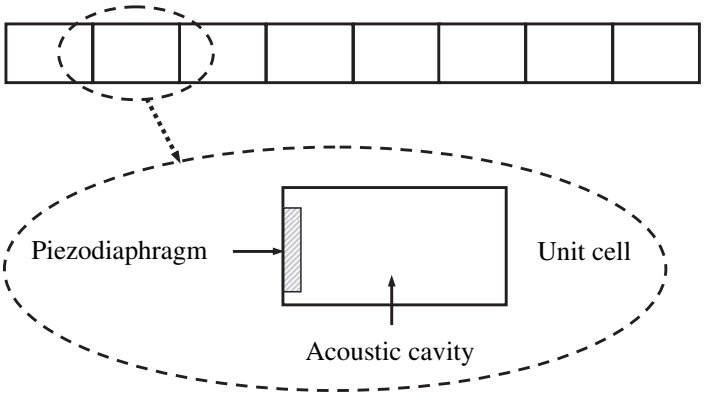

Figure 1. Configuration of the AAMM.

elastic membranes. Yao *et al* [9] have reported similar results using a mechanical analogue of Lee *et al*'s experimental prototype.

In all the above studies, the focus has been placed on passive metamaterials with fixed material properties. This limits considerably the potential of these materials. In this paper, the emphasis is placed on investigating the details of the structure of a new class of active acoustic metamaterial (AAMM) introduced by Baz [16]. In the AAMM, the effective densities can be programmed to have increasing or decreasing variation patterns along and across the material volume. With these unique capabilities, physically realizable acoustic cloaks can be achieved and objects treated with these active metamaterials can become acoustically invisible.

This paper is organized in five sections. In section 1, a brief introduction is presented. In section 2, the configuration of the AAMM is introduced. In section 3, a lumped-parameter model of cavities with piezoelectric diaphragms is developed to motivate the need for the particular structure of the AAMM in order to achieve '*programmable*' and '*tunable*' characteristics. In section 4, numerical examples are presented to illustrate the different capabilities of the AAMM and the effect of its different components on the frequency bandwidth and control voltage. A brief summary of the conclusions and outline of future work are outlined in section 5.

2. Configuration of the AAMM

Figure 1 displays a configuration of a multi-cell AAMM which consists of an array of fluid cavities separated by piezoelectric boundaries. These smart self-sensing and actuating boundaries are used to control the stiffness of the individual cavity and in turn its dynamical density through direct acoustic pressure feedback. Mechanically, each unit cell of this array is identical to other cells which make the physical realization of this concept rather feasible. However, electrically, the piezo boundaries are controlled separately in order to achieve increasing or decreasing dynamical density distributions that can also vary by many orders of magnitudes along the array.

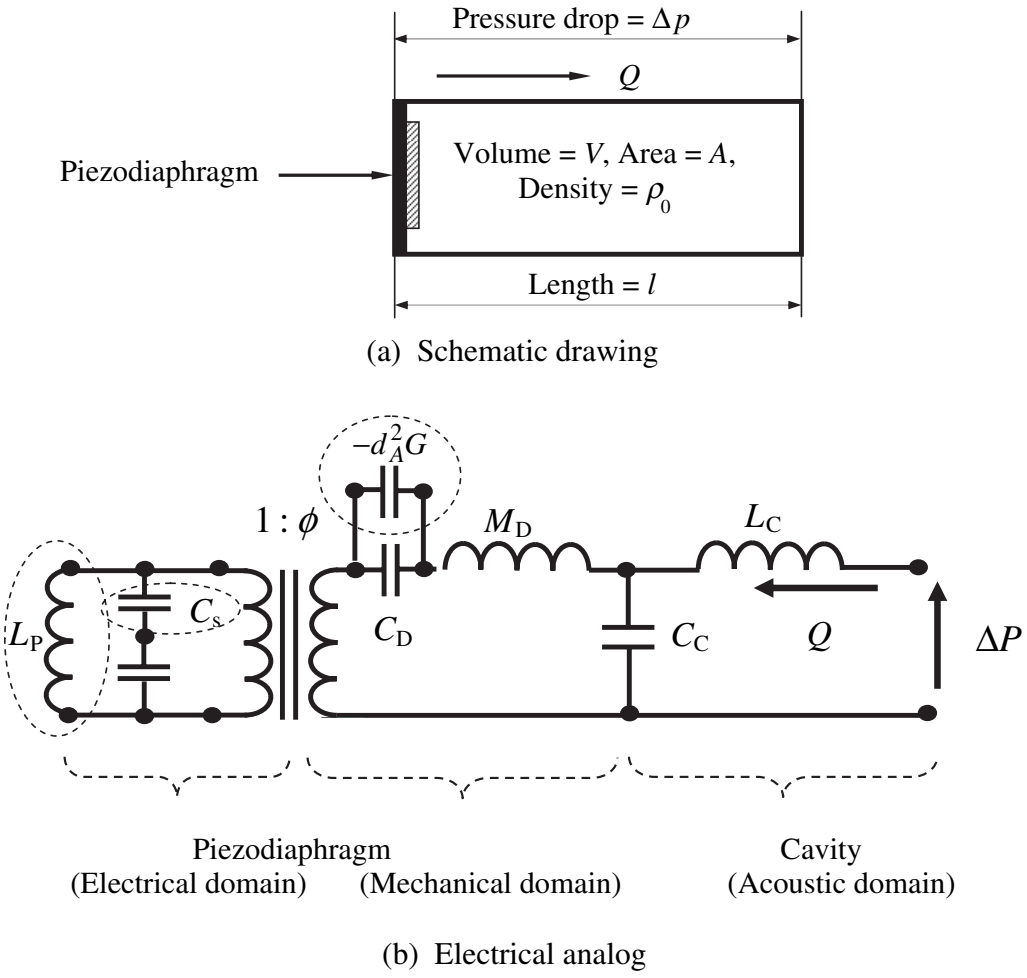

Figure 2. Acoustic cavity with piezodiaphragm.

3. Acoustic cavity with piezodiaphragm

3.1. Basic structure

Consider the basic structure of an acoustic cavity with piezoelectric diaphragm which is shown schematically in figure 2(a). The corresponding electrical analogue is displayed in figure 2(b). The basic equations that govern the modeling of the acoustic cavity and piezoelectric diaphragm by their equivalent electrical analogues are given in appendices A and B, respectively.

In figure 2(b), three components are added to the system to provide it with its desirable and tunable characteristics. These components are encircled with the dashed-line ellipses. The first of these components is active in nature which is the capacitance $(-d_{\mathrm{A}}^2 G)$ that is generated by feedback control. The other two components are passive and include the capacitance C_{s} and the inductance L_{P}. The role of each of these components and their effect on the metamaterial performance will be discussed in great detail in what follows.

3.2. Basic equations

The basic constitutive equation for a piezoelectric material is given by

$$\begin{Bmatrix} S \\ D \end{Bmatrix} = \begin{bmatrix} s^E & d \\ d & \varepsilon \end{bmatrix} \begin{Bmatrix} T \\ E \end{Bmatrix}, \tag{1}$$

where $S =$ strain, $D =$ electrical displacement, $T =$ stress, $E =$ electrical field, $s^E =$ compliance, $d =$ piezoelectric strain coefficient and $\varepsilon =$ permittivity. Equation (1) can be rewritten as

$$\begin{Bmatrix} \Delta \mathrm{Vol} \\ q \end{Bmatrix} = \begin{bmatrix} C_\mathrm{D} & d_\mathrm{A} \\ d_\mathrm{A} & 1/Z_\mathrm{P}s \end{bmatrix} \begin{Bmatrix} \Delta p_\mathrm{P} \\ V_\mathrm{P} \end{Bmatrix} \tag{2}$$

where $\Delta \mathrm{Vol} =$ change in diaphragm volume, $q =$electrical charge, $\Delta p_\mathrm{P} =$ pressure across piezodiaphragm and $V_\mathrm{P} =$ voltage. Also, $C_\mathrm{D} =$ diaphragm compliance and $Z_\mathrm{P} =$ impedance of piezodiaphragm and attached passive elements, given by

$$Z_\mathrm{P} = [(L_\mathrm{P}s)/\{1 + L_\mathrm{P}C_\mathrm{P}C_\mathrm{s}s^2/(C_\mathrm{P} + C_\mathrm{s})\}], \tag{3}$$

where $C_\mathrm{P} =$ capacitance of piezodiaphragm $= A\varepsilon/t$ with $A =$ diaphragm area and $t =$ diaphragm thickness. Also, L_P denotes a shunted inductance in-parallel with the piezodiaphragm, and C_s denotes a capacitance in-series with the piezodiaphragm.

Using the piezodiaphragm as a self-sensing actuator, then the second row of equation (2) gives, for a short-circuit piezo-sensor, the following expression:

$$q = d_\mathrm{A}\Delta p_\mathrm{P}. \tag{4}$$

Then, the voltage V_P applied to the piezodiaphragm can be generated by a direct feedback of the charge q such that

$$V_\mathrm{P} = -Gd_\mathrm{A}\Delta p_\mathrm{P}, \tag{5}$$

where $G =$ feedback gain.

Then, the first row of equation (2) yields

$$\Delta \mathrm{Vol} = C_\mathrm{D}\Delta p_\mathrm{P} - d_\mathrm{A}^2 G\Delta p_\mathrm{P} = C_\mathrm{DC}\Delta p_\mathrm{P}, \tag{6}$$

where $C_\mathrm{DC} =$ closed-loop compliance of piezodiaphragm.

Equation (6) indicates that the closed-loop compliance of piezodiaphragm (C_DC) consists of two capacitances which are connected in parallel. The first capacitance can be identified as the passive (open-loop) compliance of the diaphragm whereas the second capacitance is generated by virtue of the feedback of the pressure difference across the diaphragm.

Figure 3 displays a simplified electrical analogue of the acoustic cavity with closed-loop piezodiaphragm with the electrical components converted to their equivalent acoustical analogues.

The transfer function of the controlled cavity system, relating the flow velocity u to the pressure drop ΔP is given by

$$\frac{\Delta p}{l} = -\rho_0 \left[1 + \frac{C_\mathrm{DC}T + 1}{L_\mathrm{C}s^2(C_\mathrm{DC} + C_\mathrm{C}[C_\mathrm{DC}T + 1])}\right] su, \tag{7}$$

where

$$T = M_\mathrm{D}s^2 + Z_\mathrm{p}'s, \tag{8}$$

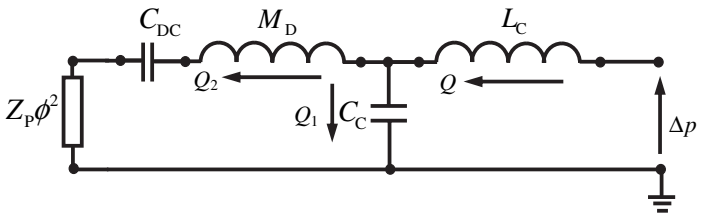

Figure 3. Simplified electrical analogue of the acoustic cavity with closed-loop piezodiaphragm.

with

$$Z'_P = Z_P\phi^2 \tag{9}$$

where $\phi = -d_A/C_D$ = electro-acoustic transduction coefficient.

Equation (7) yields the following expression for the effective density ρ_{eff}:

$$\rho_{eff}/\rho_0 = \left[1 + \frac{C_{DC}T + 1}{L_C s^2(C_{DC} + C_C[C_{DC}T + 1])}\right]. \tag{10}$$

If ρ_{eff}/ρ_0 is to assume a desired value $= \rho'_d$, then equation (10) yields the following control gain G:

$$G = \frac{(\rho'_d - 1)L_C s^2(C_C + C_D + C_C C_D T) - C_D T - 1}{d_A^2[(\rho'_d - 1)L_C s^2(1 + C_C T) - T]}. \tag{11}$$

3.3. Special cases

Several special cases of equation (10) are considered in order to demonstrate the importance of the selected structure of the AAMM shown in figure 2. Furthermore, the considered cases will emphasize the role that the added active and passive components ($-d_A^2 G$, C_S, L_P) have in shaping the spectral performance characteristics of the metamaterial.

Case 1: Passive acoustic cavity with flexible diaphragm. In this case, $G = 0$, $C_C = 0$, $M_D = 0$, $C_S = \infty$ and $L_P = 0$, and equation (10) reduces to

$$\rho_{eff}/\rho_0 = 1 + \frac{A}{l\rho_0 C_D}\frac{1}{s^2} = 1 + \frac{k_D}{\rho_0 s^2}, \tag{12}$$

where

$$k_D = \frac{A}{lC_D} = \text{diaphragm stiffness.}$$

For sinusoidal pressures, with a frequency ω, equation (12) becomes

$$\rho_{eff}/\rho_0 = 1 - \frac{k_D}{\rho_0\omega^2}. \tag{13}$$

Equation (13) indicates that the relative effective density ρ_{eff}/ρ_0 is influenced by both of the diaphragm stiffness k_D and the frequency ω. Increasing the frequency ω from 0 to ∞

makes ρ_{eff}/ρ_0 vary from $-\infty$ to a maximum value of 1. Similarly, as k_{D} is varied from 0 to ∞, ρ_{eff}/ρ_0 changes from a maximum value of 1 to $-\infty$. Note that k_{D} cannot assume negative values in order to make $\rho_{\text{eff}}/\rho_0 > 1$ because this means that the diaphragm becomes elastically unstable. Hence, passive acoustic cavities with flexible diaphragms can only generate values of $\rho_{\text{eff}}/\rho_0 \leqslant 1$ and are incapable of maintaining ρ_{eff}/ρ_0 constant except at a particular frequency. These characteristics render this class of cavities unsuitable for the practical realization of acoustic cloaks where ρ_{eff}/ρ_0 must assume and maintain any specific value between ∞ and 0 over broad frequency ranges. Such serious limitations of the passive acoustic cavities are avoided completely by adopting the concept of active acoustic cavities.

Case 2. Active acoustic cavity with piezodiaphragm. In this case, let $C_{\text{C}} = 0$ and $M_{\text{D}} = 0$; then equation (10) reduces to

$$\rho_{\text{eff}}/\rho_0 = 1 + \left[\frac{L_{\text{P}}(C_{\text{DC}}\phi^2 + C_{\text{t}})}{L_{\text{C}}C_{\text{DC}}} + \frac{1}{L_{\text{C}}C_{\text{DC}}s^2}\right]\frac{1}{(1 + L_{\text{P}}C_{\text{t}}s^2)}, \tag{14}$$

where $C_{\text{t}} = C_{\text{PB}}C_{\text{s}}/(C_{\text{PB}} + C_{\text{s}})$.

For sinusoidal pressures, with a frequency ω, equation (14) becomes

$$\rho_{\text{eff}}/\rho_0 = 1 + \left[\frac{L_{\text{P}}(C_{\text{DC}}\phi^2 + C_{\text{t}})}{L_{\text{C}}C_{\text{DC}}} - \frac{1}{L_{\text{C}}C_{\text{DC}}\omega^2}\right]\frac{1}{(1 - L_{\text{P}}C_{\text{t}}\omega^2)}. \tag{15}$$

If ρ_{eff}/ρ_0 is to assume a desired value $= \rho'_{\text{d}}$, then two sub-cases are considered

(a) $\rho'_{\text{d}} < 1$:

Equation (15) can be rewritten as

$$\omega^2 = \frac{(\rho'_{\text{d}} - 1)L_{\text{C}}C_{\text{DC}} - L_{\text{P}}(C_{\text{DC}}\phi^2 + C_{\text{t}})}{(\rho'_{\text{d}} - 1)L_{\text{C}}C_{\text{DC}}L_{\text{P}}C_{\text{t}} - 1}. \tag{16}$$

If the closed-loop compliance C_{DC} is maintained >0, in order to avoid elastic instability of the diaphragm, then both the numerator and denominator of equation (16) are negative. This indicates that ρ'_{d} can be maintained constant for any positive and real frequency ω. Note that this conclusion is also valid even when $C_{\text{S}} = \infty$ and $L_{\text{P}} = 0$. Accordingly, only the active control component capacitance $(-d_{\text{A}}^2 G)$ is needed to maintain the value of $\rho_{\text{eff}}/\rho_0 = \rho'_{\text{d}}$.

(b) $\rho'_{\text{d}} > 1$:

Equation (15) can be rewritten as

$$\rho_{\text{eff}}/\rho_0 - 1 = [L_{\text{P}}(C_{\text{DC}}\phi^2 + C_{\text{t}})\omega^2 - 1]\frac{1}{L_{\text{C}}C_{\text{DC}}(1 - L_{\text{P}}C_{\text{t}}\omega^2)\omega^2}. \tag{17}$$

Hence, $(\rho'_{\text{d}} - 1) > 0$ and the closed-loop compliance C_{DC} is maintained > 0, requires that

$$\frac{1}{L_{\text{P}}(C_{\text{DC}}\phi^2 + C_{\text{t}})} < \omega^2 < \frac{1}{L_{\text{P}}C_{\text{t}}}. \tag{18}$$

Equation (18) sets the bounds on the frequency range for which $\rho'_{\text{d}} - 1 > 0$. Note that the upper bound of this frequency ranges can be increased by reducing both L_{P} and C_{t}. The frequency band between the upper and lower bounds is defined as the '*bandwidth*' of the AAMM.

Note that the presence of L_{P} is essential for $(\rho'_{\text{d}} - 1) > 0$ as it makes the numerator of equation (18) positive. However, if $L_{\text{P}} = 0$, the numerator will always be negative and $\rho'_{\text{d}} > 1$ cannot be achieved.

Table 1. Role of the components added to the AAMM.

No.	Component	Role
1	Active capacitance $-d_A^2 G$	Ensures that ρ_d' can be maintained constant over a desired frequency range
2	Passive inductance L_P	Ensures that $\rho_d' > 1$ can be achieved
3	Passive capacitance C_S	Enhances the frequency bandwidth of the metamaterial

Table 2. Parameters of acoustic cavity/piezodiaphragm system [17].

Parameter	Value
ϕ	$138.3\,\mathrm{Pa\,V^{-1}}$
C_D	$1.5243 \times 10^{-13}\,\mathrm{m^4 s^2\,kg^{-1}}$
M_D	$13\,456\,\mathrm{kg\,m^{-4}}$
d_A	$-2.1080 \times 10^{-11}\,\mathrm{m^3\,V^{-1}}$
C_{PB}	18.239 nF
C_C	$1.8466 \times 10^{-15}\,\mathrm{m^4 s^2\,kg^{-1}}$
L_C	$24\,069\,\mathrm{kg\,m^{-4}}$

Therefore, it is necessary that the structure of the AAMM must include the shunting inductance L_P to ensure that $\rho_d' > 1$. Furthermore, the effective bandwidth of operation of the AAMM can be enhanced by the addition of the passive capacitance C_S as implied by equation (18). Table 1 summarizes the role of the three components which are added to the structure of the AAMM shown in figure 2. Numerical examples are presented in section 4 to illustrate the influence of the different components of the AAMM on its overall performance.

4. Effect of structure of the AAMM on its performance

Consider an acoustic cavity with a piezodiaphragm that has the characteristics listed in table 2 (Parasad *et al* [17]).

Figure 4 shows typical performance characteristics of the AAMM when $\rho_d' = 20$, $L_P = 50\,\mathrm{H}$, and $C_S = 0.2\,\mathrm{pf}$. Under these conditions, the AAMM has an '*operating frequency bandwidth*' of 48 950 Hz as shown in figure 4(c). Beyond that bandwidth, the closed-loop compliance C_{DC}, in $\mathrm{m^4 s^2\,kg^{-1}}$, becomes negative indicating that the AAMM becomes elastically unstable.

Figure 4(a) indicates that the AAMM can maintain the relative density ρ_d' at 20 while requiring the input control voltage displayed in figure 4(b).

The effect of the inductance L_P and the capacitance C_S on the effective bandwidth of the AAMM is shown in figure 5. Figure 5(a) displays the contours of the iso-frequency bandwidth of the AAMM in the L_P–C_S plane, for $\rho_d' = 20$.

For example, an iso-frequency bandwidth line that has a value of 0.5×10^4 Hz defines all the designs of the AAMM that have frequency bandwidth of 0.5×10^4 Hz. Such designs can be obtained by providing the AAMM with $L_P = 1000\,\mathrm{H}$ and $C_S = 1\,\mathrm{pf}$, or with $L_P = 200\,\mathrm{H}$ and $C_S = 5.2\,\mathrm{pf}$.

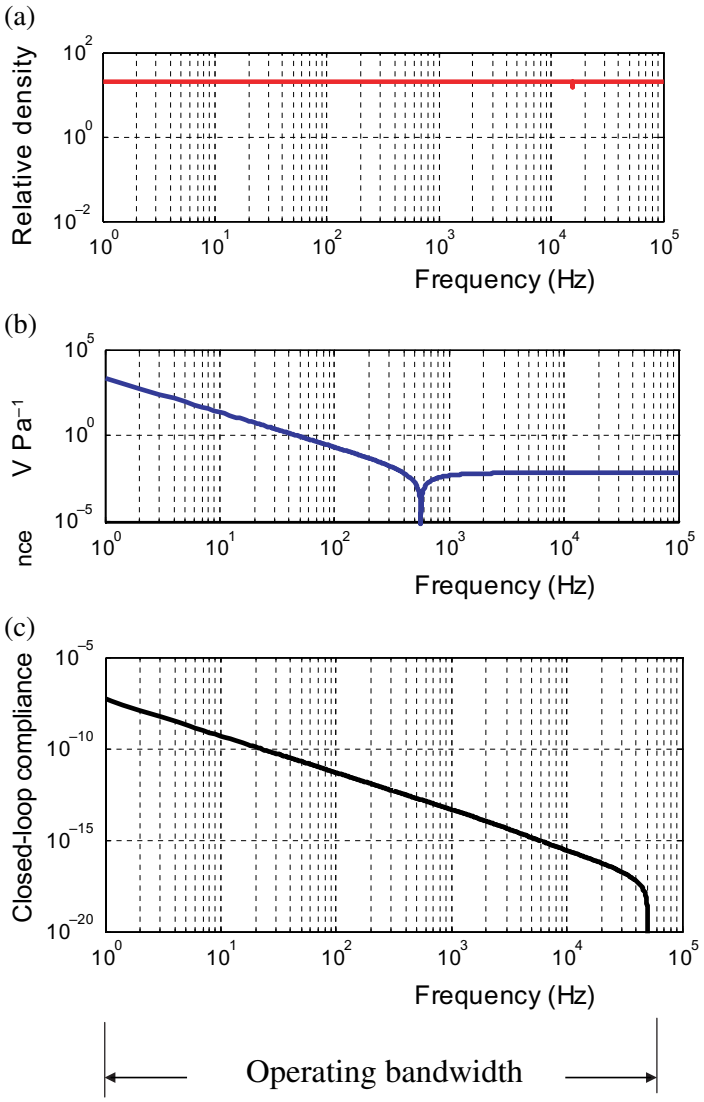

Figure 4. Typical performance of the AAMM.

The displayed results suggest that decreasing both L_P and C_S is essential to enhancing the frequency bandwidth of the material. However, decreasing either L_P or C_S can also improve the frequency bandwidth.

Figures 5(b) and (e) show the frequency response profiles of the closed-loop compliance for values of L_P (in H) and C_S (in pf) of (1000,10), (50,1), (1000,0.2) and (50, 0.2), respectively. The effect of decreasing L_P and C_S on extending the bandwidth of operation of the metamaterial is evident.

Table 3 summarizes a comparison between the upper and lower bounds of the effective frequency band of the metamaterial as predicted by equation (18) and by the zones for which the closed-loop compliance is positive in order to avoid elastic instability of the piezodiaphragm. Close agreement between these two methods is evident from table 3.

Figure 6(a) displays the effect of the inductance L_P and the capacitance C_S on the contours of the iso-control V Pa^{-1} of the AAMM for $\rho'_d = 20$. The displayed results suggest

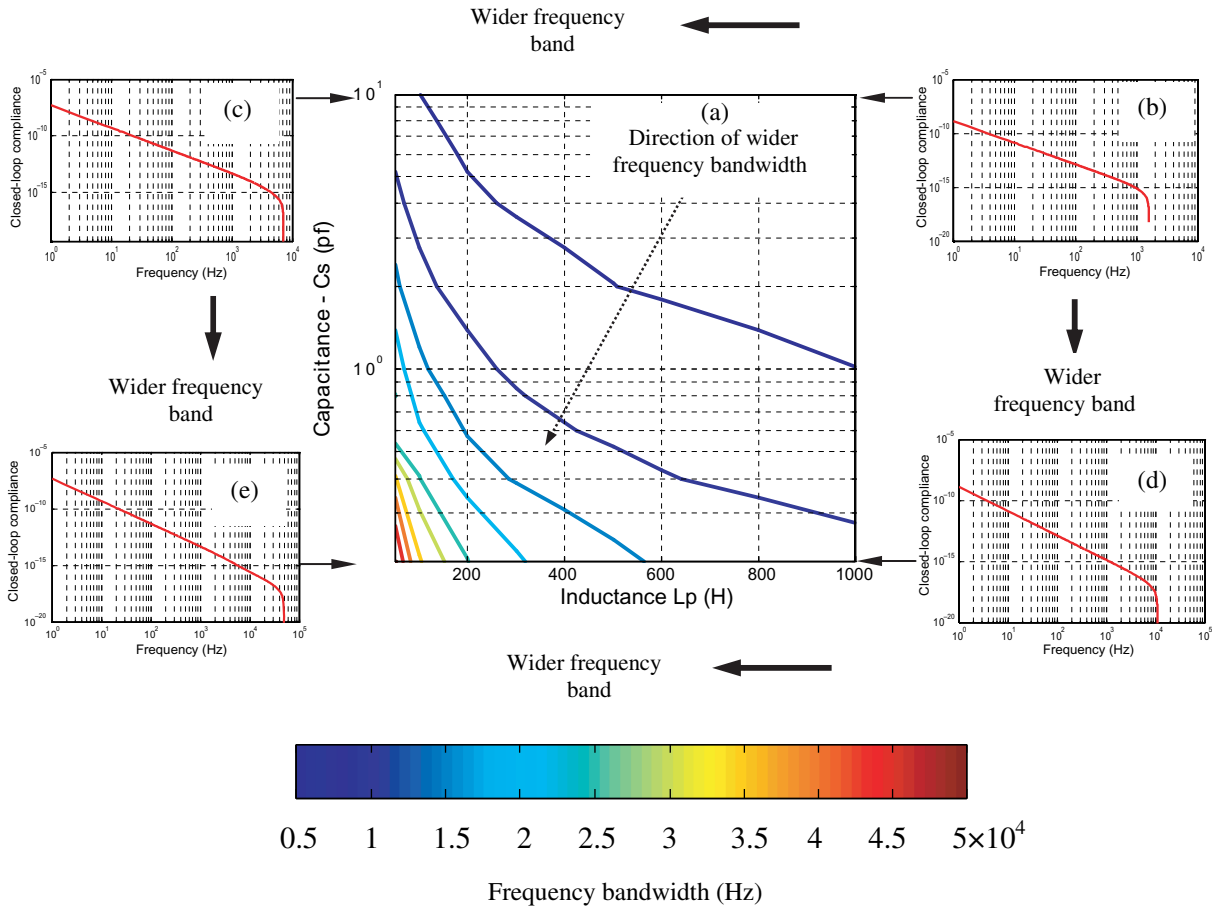

Figure 5. Effect of the inductance L_P and the capacitance C_S on the contours of the iso-frequency bandwidth of the AAMM.

Table 3. Predictions of upper and lower bounds of frequency band of the metamaterial.

L_P (H) and C_S (pf)	(1000,10)	(50,10)	(1000,0.2)	(50,0.2)
Upper Limit (Hz)				
Equation (18)	1592	7119	11 210	48 900
$C_{DC} > 0$	1592	7115	11 254	48 950
Lower limit (Hz)				
Equation (18)	2.400	2.470	2.477	1.835
$C_{DC} > 0$	0	0	0	0

that decreasing L_P increases the control voltage whereas C_S has virtually no effect on the control voltage.

Figures 6(b) and (c) show the frequency response profiles of the control voltage for values of L_P (in H) and C_S (in pf) of (1000,0.2) and (50,0.2), respectively. It is evident that decreasing L_P reduces the control voltage of the metamaterial which is necessary to maintaining $\rho'_d = 20$.

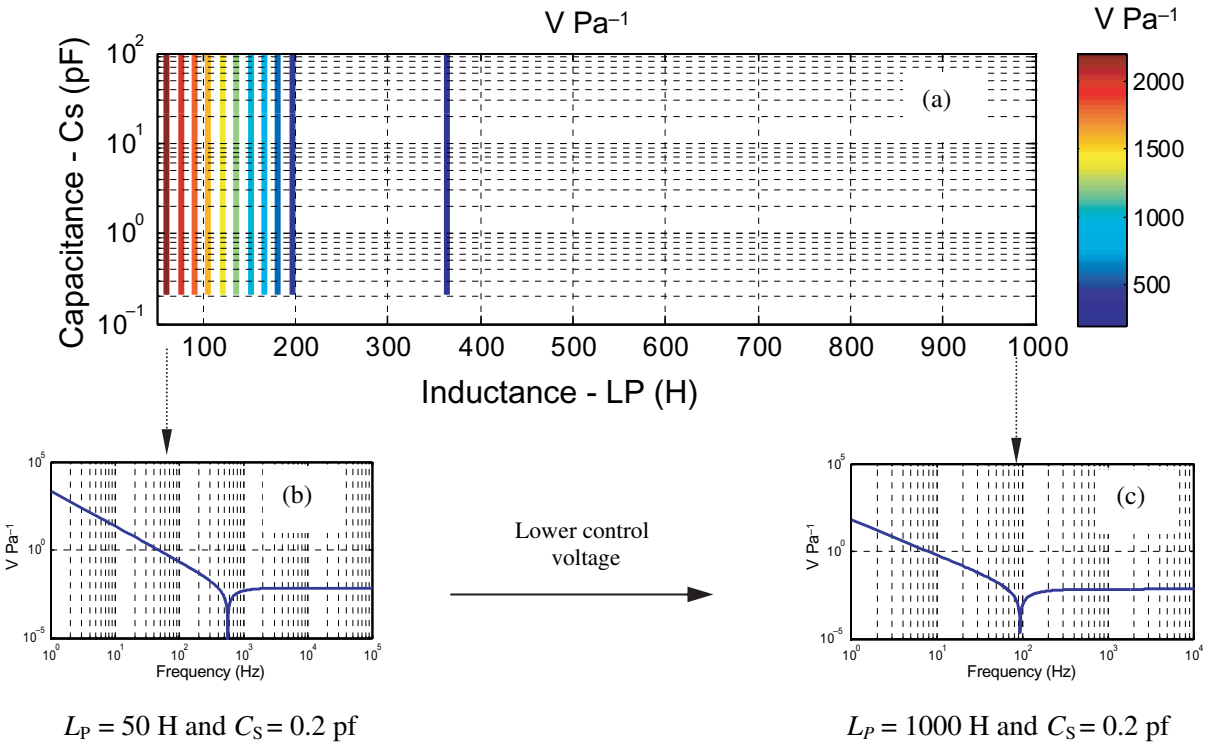

Figure 6. Effect of the inductance L_P and the capacitance C_S on control voltage of the AAMM.

Figure 5 indicates that increasing the frequency bandwidth of the metamaterial requires that L_P to be small but at the expense of increasing the control voltage as shown in figure 6.

Considering a performance index (PI) which is defined as

$$\text{PI} = \text{Frequency bandwidth}/(\text{control voltage Pa}^{-1}). \tag{19}$$

Maximizing this PI ensures that the frequency bandwidth is maximized while the control voltage is minimized. Figure 7 displays the effect of the inductance L_P and the capacitance C_S on the iso-performance index contours. For the considered ranges of L_P and C_S, PI attains a maximum at $L_P = 1000$ H and $C_S = 0.2$ pf resulting in a frequency bandwidth of 11 254 Hz and control voltage of 64.3 V Pa^{-1}. Note that maximizing the frequency bandwidth alone results in a bandwidth of 50 000 Hz but a control voltage of 2345 V Pa^{-1}. This bandwidth is 4.47 times that resulting from maximizing the PI but the control voltage is 36.47 times that obtained by maximizing PI.

5. Conclusions

This paper has presented a detailed analysis of the structure of a new class of one-dimensional acoustic metamaterials with programmable densities. The AAMM is shown to be theoretically capable of generating densities that are orders of magnitudes lower and higher than the ambient fluid. Such capabilities are achieved by using an array of fluid cavities separated by piezoelectric boundaries which are controlled actively to generate constant densities over broad frequency bands. Furthermore, the piezo boundaries are augmented with passive electrical components

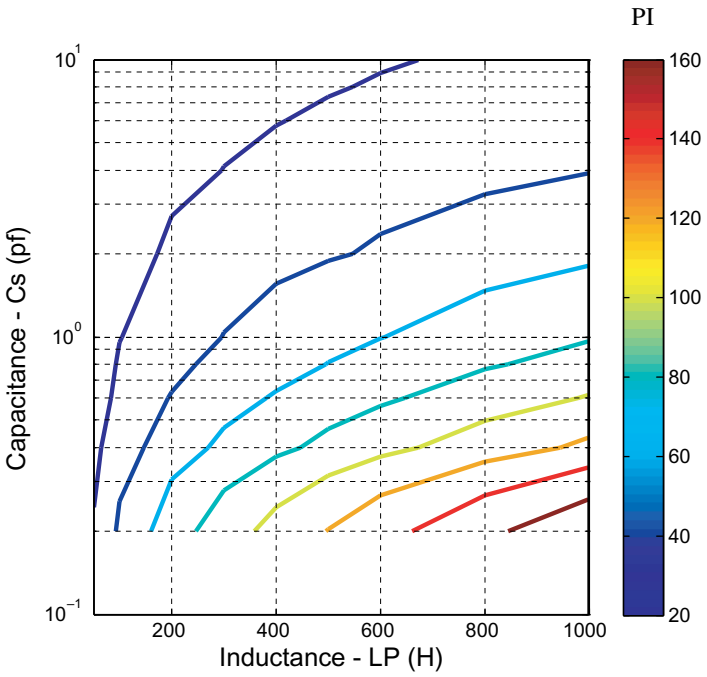

Figure 7. Effect of the inductance L_P and the capacitance C_S on the PI of the AAMM.

to enhance the frequency bandwidth of operation and enable the generation of densities which are orders of magnitudes higher than the ambient medium. The addition of these components is found to be essential to avoid the elastic instability of the piezo boundaries. Selection of the values of the passive components, on a rational basis, is presented in order to ensure a balance between the frequency bandwidth and control voltage.

Comparisons are also presented between the characteristics of the active and passive metamaterials to emphasize the potential of the active metamaterials for physically generating a wide range of effective densities in a simple and uniform manner.

A natural extension of this work is to extend the presented 1D lumped-parameter model of the AAMM to a 2D model. Also, work is now in progress to include active control capabilities to tailor the bulk modulus distribution of the metamaterial. Combining the tunable density and bulk modulus capabilities will enable the physical realization of practical acoustic cloaks and objects treated with these active metamaterials can become acoustically invisible. Experimental prototypes of the AAMM are now being manufactured to demonstrate the feasibility of the concept and to evaluate its merits and limitations.

Acknowledgments

This work has been funded by a grant from the Office of Naval Research (N000140910038). Special thanks are due to Dr Kam Ng and Dr Scott Hassan, the technical monitors, for their invaluable input and comments.

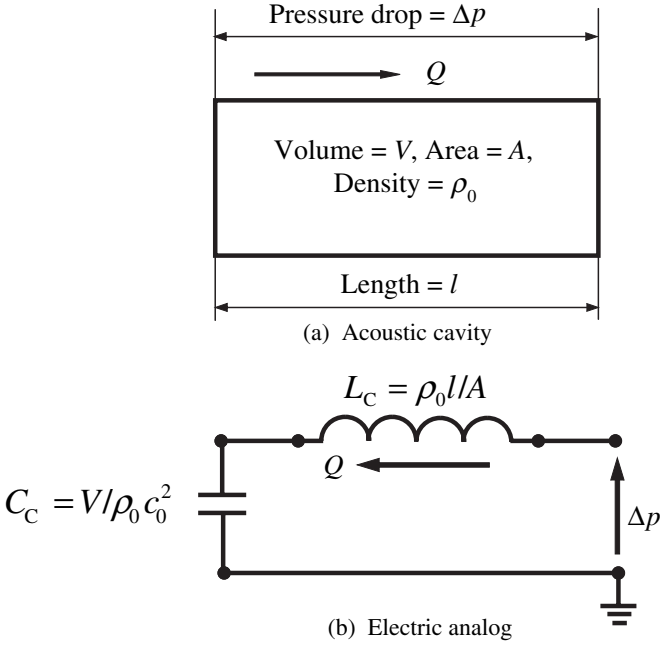

Figure A.1. Closed acoustic cavity and its electrical analogue.

Appendix A. Electrical analogue of an acoustic cavity

The acoustic cavity, shown in figure (A.1), is modeled using its electrical analogue. This analogue can be easily coupled with the electrical analogue of the piezoelectric diaphragm. In this regard, the acoustic cavity model is developed using a lumped-parameter approach which is valid when the wavelength of the acoustic waves is much greater than the cavity dimensions [18]. The lumped-parameter approach suggests that the cavity is equivalent to a spring-mass system which electrically is equivalent to a capacitance C_C and inductance L_C.

It can be easily shown that the capacitance C_C and inductance L_C are given by [18]

$$C_C = V/\rho_0 c_0^2 \quad \text{and} \quad L_C = \rho_0 l/A \tag{A.1}$$

where V = volume of cavity, A = cross-sectional area of cavity, l = cavity length, ρ_0 = density of fluid inside cavity, and c_0 = speed of sound.

Appendix B. Electrical analogue of piezoelectric diaphragm

The constitutive equation of the piezodiaphragm alone without any added electrical components can be obtained from equation (2) as follows:

$$\begin{Bmatrix} \Delta \mathrm{Vol} \\ q \end{Bmatrix} = \begin{bmatrix} C_D & d_A \\ d_A & C_P \end{bmatrix} \begin{Bmatrix} \Delta p_P \\ V_P \end{Bmatrix}. \tag{B.1}$$

Equation (B.1) can be differentiated with respect to time to yield

$$\begin{Bmatrix} Q \\ i \end{Bmatrix} = \begin{bmatrix} C_D s & d_A s \\ d_A s & C_P s \end{bmatrix} \begin{Bmatrix} \Delta p_P \\ V_P \end{Bmatrix}, \tag{B.2}$$

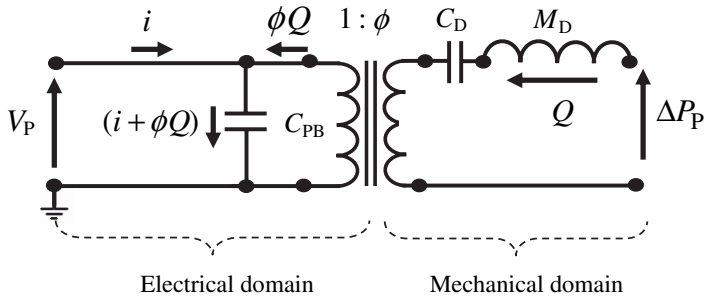

Figure B.1. Electrical analogue of the piezoelectric diaphragm.

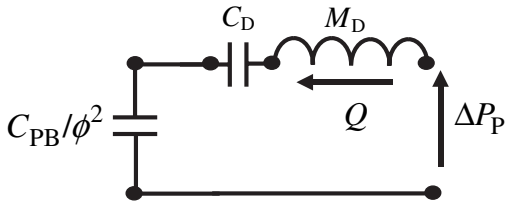

Figure B.2. Simplified electrical analogue of the piezoelectric diaphragm.

where Q = the rate of volumetric changes = $\mathrm{d}\Delta\mathrm{Vol}/\mathrm{d}t$, i = current = $\mathrm{d}q/\mathrm{d}t$ and s = Laplace complex number. Multiplying the first row of equation (B.2) by ϕ and adding it to the second row gives

$$(i + \phi Q) = C_{\mathrm{PB}} s V_{\mathrm{P}} \tag{B.3}$$

where $C_{\mathrm{PB}} = (1 - k^2)C_{\mathrm{P}}$ = blocked capacitance of the piezodiaphragm with $k^2 = d_{\mathrm{A}}^2/C_{\mathrm{D}}C_{\mathrm{P}}$. Note that k^2 is defined as the electro-acoustic coupling factor. Equation (B.3) represents the flow of the current $(i + \phi Q)$ through the capacitance C_{PB} due to an applied voltage V_{P}. This can be schematically represented by the electrical circuit shown in left half of figure (B.1) to describe the physics of the electrical domain of the piezodiaphragm.

Accordingly, the electrical analogue of the piezoelectric diaphragm can be simplified as shown in figure (B.2).

In this figure, it can be seen that the pressure difference ΔP_{P} across the piezoelectric diaphragm counterbalances the inertia of the diaphragm M_{D}, its mechanical compliance C_{D}, and the mechanical compliance (C_{PB}/ϕ^2) which is equivalent to the piezoelectric capacitance C_{PB}.

Note that the piezoelectric capacitance C_{PB} is related to the voltage V_{P} and current i_{P} as follows:

$$V_{\mathrm{P}} = \frac{1}{C_{\mathrm{PB}}} \int i_{\mathrm{P}} \mathrm{d}t. \tag{B.4}$$

To determine the equivalent mechanical impedance, the basic equations of the electro-acoustic transduction coefficient ϕ are used. These basic equations are given by

$$\Delta P_{\mathrm{P}} = \phi V_{\mathrm{P}} \tag{B.5}$$

and

$$Q = \frac{1}{\phi} i_{\mathrm{p}}. \tag{B.6}$$

In effect, these equations make the piezodiaphragm act as a transformer of the electric energy into acoustic energy with a transformer turning ratio $= \phi$. During this energy transformation process, the voltage is amplified by ϕ and the current is reduced by ϕ while the total power $V_{\mathrm{P}} i_{\mathrm{P}} = \Delta P_{\mathrm{P}} Q$. Hence, equations (B.4) through (B.6) yield

$$\frac{\Delta P_{\mathrm{P}}}{\phi} = \frac{1}{C_{\mathrm{PB}}} \int \phi Q \mathrm{d}t, \tag{B.7}$$

or

$$\Delta P_{\mathrm{P}} = \frac{1}{C_{\mathrm{PB}}/\phi^2} \int Q \mathrm{d}t. \tag{B.8}$$

Equation (B.7) indicates that the mechanical compliance (C_{PB}/ϕ^2) is equivalent to the piezoelectric capacitance C_{PB}.

References

[1] Torrent D and Sanchez-Dehesa J 2007 Acoustic metamaterials for new two-dimensional sonic devices *New J. Phys.* **9** 323

[2] Torrent D and Sanchez-Dehesa J 2008 Anisotropic mass density by two-dimensional acoustic metamaterials *New J. Phys.* **10** 063015

[3] Cervera F, Sanchis L, Sanchez-Pérez J V, Martinez-Sala R, Rubio C, Meseguer F, López C, Caballero D and Sánchez-Dehesa J 2001 Refractive acoustic devices for airborne sound *Phys. Rev. Lett.* **88** 023902

[4] Krokhin A A, Arriaga J and Gumen L N 2003 Speed of sound in periodic elastic composites *Phys. Rev. Lett.* **91** 264302

[5] Torrent D, Hakansson A, Cervera F and Sanchez-Dehesa J 2006 Homogenization of two-dimensional clusters of rigid rods in air *Phys. Rev. Lett.* **96** 204302

[6] Farhat M, Enoch S, Guenneau S and Movchan A B 2008 Broadband cylindrical acoustic cloak for linear surface waves in a fluid *Phys. Rev. Lett.* **101** 134501

[7] Chan C T, Jensen L I and Fung K H 2006 On extending the concept of double negativity to acoustic waves *J. Zhejiang Univ. Sci.* A **7** 24–8

[8] Milton G W and Willis J R 2006 On modifications of Newton's second law and linear continuum elastodynamics *Proc. R. Soc.* A **463** 855–80

[9] Yao S, Zhou X and Hu G 2008 Experimental study on negative effective mass in a 1D mass–spring system *New J. Phys.* **10** 043020

[10] Huang H H, Sun C T and Huang G L 2009 On the negative effective mass density in acoustic metamaterials *Int. J. Eng. Sci.* **47** 610–17

[11] Berryman J G 2006 Effective medium theories for multicomponent poroelastic composites *J. Eng. Mech.* **132** 519–31

[12] Pendry J B and Li J 2008 An acoustic metafluid: realizing a broadband acoustic cloak *New J. Phys.* **10** 115032

[13] Norris A N 2009 Acoustic metafluids *J. Acoust. Soc. Am.* **125** 839–49

[14] Lee S H, Park C M, Seo Y M, Wang Z G and Kim C K 2009a Negative effective density in an acoustic metamaterial arXiv:0812.2954v3 [cond-mat]

[15] Lee S H, Park C M, Seo Y M, Wang Z G and Kim C K 2009b Reverse Doppler effect of sound arXiv:0901.2772v2 [cond-mat]

[16] Baz A 2009 An active acoustic metamaterial with tunable effective density *ASME J. Vib. Acoust.* in press

[17] Prasad S, Gallas Q, Horowitz S, Homeijer B, Sankar B V, Cattafesta L N and Sheplak M 2006 Analytical electroacoustic model of a piezoelectric composite circular plate *AIAA J.* **44** 2311–18

[18] Blauert J and Xiang N 2008 *Acoustics for Engineers* (Berlin: Springer)